PHYSICAL REVIEW B VOLUME 29, NUMBER 10 15 MAY 1984

Thermal conductivity of amorphous germanium at low temperatures

J. E. Graebner and L. C. Allen
AT&T Bell Laboratories, Murray Hill, New Jersey 07974
(Received 28 October 1983)

The thermal conductivity of free-standing films of *a*-Ge has been measured in the temperature range 0.03—5 K. The films were prepared by evaporation under a variety of conditions to obtain various densities, thicknesses, and impurity levels. The data can be accounted for by scattering of the thermal phonons from two-level tunneling systems, cylindrical inhomogeneities, and the boundaries of the sample. The strengths of the first two scattering mechanisms are found to be correlated inversely with the mass density of the film. The two-level tunneling systems are therefore associated predominantly with the defect regions of the material.

I. INTRODUCTION

The tetrahedrally bonded amorphous semiconductors *a*-germanium and *a*-silicon have been the subjects of a great deal of both fundamental and practical research in recent years. Many properties have been found to depend sensitively on the microscopic structure which is now known to be inhomogeneous—regions of high, nearly crystalline density are interspersed with regions of lower density. In the present work, we address the specific structural question of whether *a*-Ge supports the two-level atomic tunneling systems (TLS) which are known to exist generally in glasses.[1] These TLS are the localized configurational states which dominate the properties of glasses at low temperatures, $T \lesssim 1$ K. A number of low-temperature studies of *a*-Ge and *a*-Si have been carried out, but the interpretations have been contradictory. Measurements of the low-frequency dielectric constant[2] in sputtered *a*-Si, the thermal conductivity[3] κ of evaporated *a*-Ge, surface-acoustic-wave propagation[4] in sputtered *a*-Ge, and the heat capacity[5] of evaporated *a*-Ge have been interpreted as evidence for TLS, whereas measurements of heat capacity in sputtered[6] and evaporated[7] *a*-Ge, surface acoustic waves[8] in sputtered *a*-Si, and κ (Ref. 9) of evaporated *a*-Ge have been interpreted as evidence against the existence of TLS.

In the present study we have tried to overcome some of the limitations of previous measurements[3] of the thermal conductivity in *a*-Ge. We have lifted the films free of the substrate before cooling to liquid-helium temperatures to avoid (1) the problems of differential contraction while cooling, and (2) parallel heat conduction through sample and substrate during the measurement. We have extended the temperature range to temperatures as low as 30 mK in order to assess the contributions of various scattering mechanisms. Finally, we have used samples prepared under a variety of conditions and characterized by measurements of mass density, electrical conductivity, optical transmission, and Raman scattering. Impurity levels were determined by neutron-activation analysis, secondary-ion-mass spectroscopy (SIMS), and evolution of gases during heating. Surface texture was studied by scanning electron microscopy (SEM).

The thermal-conductivity data for all our samples can be explained by scattering of the heat carriers (thermal phonons) from TLS, cylindrical inhomogeneities, and the surface of the films. The strengths of the first two mechanisms are found to be correlated inversely with the average mass density. Thus we conclude that the TLS are associated predominantly with the low-density or defect regions of the material. This dependence on density may account for the previous contradictory results in *a*-Ge and *a*-Si. It also points out the need for careful characterization of samples, a need which has been recognized for some time in the high-temperature ($T > 1$ K) investigations in *a*-Ge and *a*-Si, but not at all in the low-temperature studies. The central features of the present investigation have been reported previously.[10]

II. EXPERIMENTAL TECHNIQUE

Most of the films were prepared by evaporation of 99.9999%-pure Ge in an ion-pumped high-vacuum system with a base pressure $P_b \sim 10^{-8}$ Torr, and a pressure during evaporation $P_e \sim 10^{-7}$ Torr. Residual gas contaminants detected by a quadrupole spectrum analyzer during a typical evaporation were N and H at partial pressures of 4×10^{-8} and 2×10^{-8} Torr, respectively. Oxygen pressure was $\lesssim 4\times10^{-9}$ Torr. To maintain the low pressure during evaporation a liquid-nitrogen-cooled copper box (15 cm on a side) shielded the sample plate on five sides. The Ta-Nb heater[11] and the vitreous carbon crucible[12] were nearly surrounded by a water-cooled copper enclosure to avoid heating other parts of the system by radiation. A thickness monitor[13] was used to measure the deposition rate and the thickness of the sample. The temperature of the copper plate holding the substrates was maintained by a tungsten lamp. The first sample to be measured was prepared in a similar vacuum system by electron-beam evaporation from a water-cooled copper hearth. This system did not have any of the cold shields of the previous system, and both P_b and P_e were at least an order of magnitude higher. The distance from source to substrate (normal incidence) was 30 cm in both systems.

TABLE I. Film characteristics for samples 1–6 and the thickest sample (LS) of Ref. 3: temperature of the sample plate T_p (°C), pressure during evaporation P_e (10^{-7} Torr), deposition rate $\dot{t}$ (Å/sec) thickness t (μm), mass density ρ (g/cm^3), electrical conductivity σ (10^{-3} Ω^{-1}cm^{-1}), and oxygen, carbon, and hydrogen concentrations (at. %).

Sample		T_p	P_e	$\dot{t}$	t	ρ	σ	c(O)	c(C)	c(H)
●	1		50	25	10.7	5.17	3.89	3		
△	2	130	1.4	10	11.2	4.88	2.00	0.24	0.17	
■	3	90	1.5	11	10.4	4.75	2.63	0.10	0.09	
○	4	80	1.2	14	13.6	4.92	1.47	0.05	0.20	0.05
□	5	100	15	11	10.3	4.88	2.13	1.5	0.24	0.05
▲	6	120	0.5	8	10.5	4.54	1.98	0.15	0.20	0.05
	LS	25			5.7		10.0			

Free-standing films for thermal-conductivity measurements were obtained by using (2.5×7.5)-cm^2 glass microscope slides coated with B_2O_3 (a parting agent) as substrates. The B_2O_3 was evaporated onto the substrate in a separate vacuum system to a thickness of ≈ 0.1 μm. Three slides were clamped against the sample plate held at temperature T_p. We present data below which suggest that the temperature at the surface of the substrate T_s was higher than T_p and depended on other parameters such as evaporation rate and clamping force.

Table I shows deposition conditions for six samples. P_e was $\sim 10^{-7}$ Torr for most samples except the first, which was prepared in the electron-gun evaporation system, and sample 5, which was made purposely at high pressure ($P_e \approx 10^{-6}$ Torr) in order to assess the role of vacuum contamination. It was found that T_p values lower than 90 °C resulted in peeling of thick (> 6 μm) films, and also that T_p values higher than ~ 140 °C resulted in microcrystallinity appearing as slightly sharpened peaks in the otherwise broad x-ray-diffraction pattern. In order to obtain thick films in a relatively short period of time and to minimize contamination, a rate of ~ 10 Å/sec was used. The final thicknesses were in the range of 10–14 μm. Thinner films were difficult to lift without breaking and thicker films had a substantial cloudiness of the exposed surface which became visible at about 8 μm and increased with thickness. We note that sample 5 exhibited more cloudiness than others. Since this film was prepared under higher P_e, the cloudiness may be related to impurity concentration.

To determine the effect of preparation conditions on the structure and other properties of the films, a number of measurements were made. The surfaces of the films were examined with a scanning electron microscope using up to 10^4 magnification. Domelike structures of average diameter ~ 1 μm were revealed. The number of these structures was correlated with cloudiness and covered up to 5% of the surface area for sample 5. Examination of the edges of broken films showed that these domes were the tops of long, thin cones embedded in the film to a depth of a few micrometers. Similar cones have been observed in other amorphous films, e.g., a-Si:H,[14] where it was suggested that they are regions of faster growth nucleated at dust or other imperfections of the substrate. The films were examined on both faces for crystallinity by Raman spectroscopy. The strongest Raman peak in a single crystal of Ge could not be detected in the films with a sensitivity of 10^{-3} times the peak height in the crystal. This absence of crystallinity confirmed our x-ray-diffraction analysis. The mass density ρ (Table I) was determined by weighing a small (~ 1 mg) piece of the lifted film in a microgram balance, using an optical microscope and planimeter to find the area, and measuring the thickness with a scanning electron microscope. The total error in ρ is estimated to be ± 2–3 %. The density ranges between 85% and 98% of the crystalline density ρ_c. Table I shows that ρ is not as well correlated with T_p as might be expected from the literature[15] assuming that $T_s \approx T_p$. Better correlation of ρ with T_s is noted if T_s is assumed to exceed T_p by an amount which depends on the deposition rate. The highest levels of oxygen are found in samples 1 and 5, which therefore correlates with higher P_e. Strong interference fringes in the infrared and visible transmission spectra precluded the observation of characteristic absorption bands. The index of refraction n was determined from the fringe spacing and the thickness, which was measured on the same piece with a scanning electron microscope. It shows the same general dependence on photon energy as films prepared by evaporation under similar vacuum conditions,[16] or sputtered[17] at comparable substrate temperatures. The absorption was deduced by using n and trial values of α to match a calculated transmission fringe pattern[18] to the pattern observed. The absorption edges are all relatively sharp, and in this respect are typical of unannealed a-Ge.[19–21] The two samples with high oxygen concentration, however, have the highest absorption. This is in contrast to studies[22,23] at lower oxygen levels where the oxygen shifted the absorption edge to higher energies. The values of n for high oxygen levels are also larger than is typical, especially at high photon energies. However, samples 2–4 and 6, prepared under cleaner conditions, agree quite well at 0.2 eV with sputtered samples[15] of various densities (Fig. 1). We attribute the variation of n to the competing effects in this material of density and impurity level. The same pattern is observed for $\alpha(\rho)$ in Fig. 1. Room-temperature electrical conductivity measurements were performed using Au pads and heaters (see below) as electrodes. No significant change was observed as a result of heating to 100 °C in air for several minutes to facilitate ultrasonic bonding[24] of the Au wires to the Au pads. The values of electrical conductivity are typical for evaporated a-Ge.

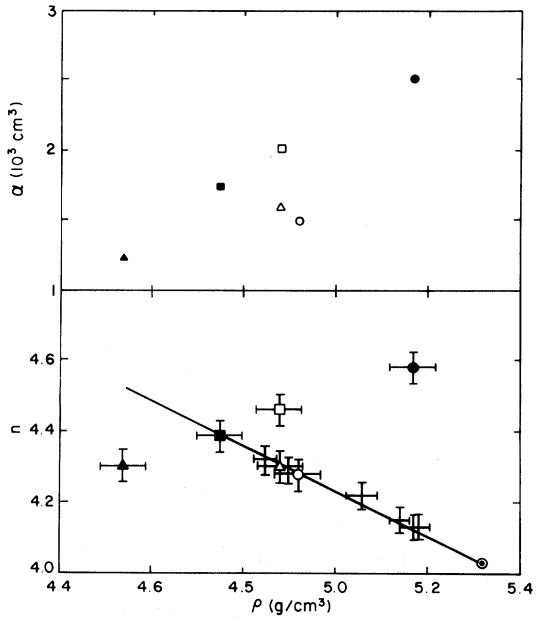

FIG. 1. Optical absorption α at $\hbar\omega=0.75$ eV and index of refraction n at $\hbar\omega=0.2$ eV vs average mass density of a-Ge films. All data were obtained at room temperature. Results for n of unannealed films (Ref. 15) are shown by crosses without symbols.

Pieces of one sample (no. 3) were annealed for 1 h at various temperatures $T_a=210$, 310, and 350 °C. The film thickness was found to decrease with increasing T_a ($\sim 12\%$ for $T_a=310$ °C, consistent with its density deficit of 11%). Crystallization took place only at 350 °C and was explosive in nature.

Thin-film manganin heaters and isothermal Au pads for the measurement of thermal conductivity[25] were deposited by evaporation onto the films in a separate vacuum system using masks to form the pattern shown in Fig. 2. The use of two heaters and one thermometer has the advantages of (1) precise definition of the active sample region by the thin-film heaters, and (2) the need for only a single thermometer calibration. After electrical and thermal leads were attached, the film was floated off the substrate by immersion in water for ~ 1 h to dissolve the B_2O_3, and then mounted with the leads under slight tension in a ^{3}He-^{4}He dilution refrigerator.

The thermal-conductivity measurement used a thermal gradient across a narrow region of the Ge film delineated by the heaters. The measurement was made in the following way. A flow of heat $\dot{Q}$ was generated electrically in the heater closer to the thermal sink, raising the thermometer to temperature T_1. The electrical current was then switched to the other heater and adjusted (in case of slightly different heater resistances) to give the same $\dot{Q}$, raising the thermometer to $T_2>T_1$. Then $\kappa=(L/A)\dot{Q}(T_2-T_1)$, where the effective length L for heat flow was determined experimentally to be the center-to-center separation of the heaters. The cross-sectional area $A=wt$, where $w=1$ cm (Fig. 2) and t was the sample thickness (Table I).

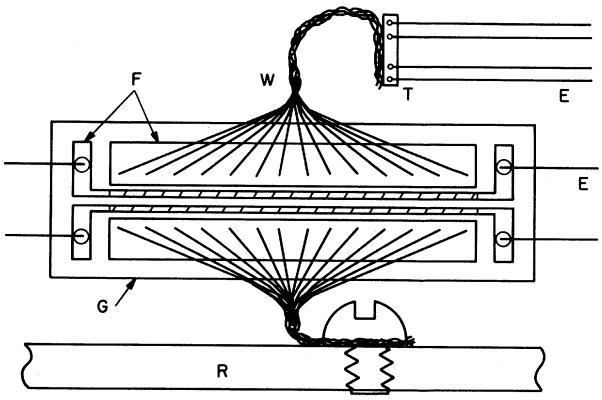

FIG. 2. Schematic diagram of a thermal-conductivity sample. Gold pads (F) ~ 1 μm thick are deposited over a thin layer of Cr on the sample (G) of a-Ge. Nb-Ti leads 0.0015 cm in diameter (E) are soldered to the thermometer (T) and to the gold pads (F) for the manganin heaters (cross-hatched area) which are 0.015 cm wide, 1 cm long and ~ 500 Å thick. Thermal connections are made to thermometer and refrigerator (R) by means of 25-μm diam Au wires ultrasonically bonded to the Au pads.

The geometrical arrangement of pattern 1 (samples 2, 3, and 6) with its large area/length ratio is expected to minimize end effects. In this pattern, shown in Fig. 2, the heaters have a center-to-center spacing $s=0.040$ cm. Data for samples 1, 4, and, 5 were taken using pattern 2, with $s=0.075$ cm. Correction for end effects should be more important for this pattern. To obtain a correction factor, κ was measured using both patterns on neighboring portions of the same film. Pattern 2 was found to give $\sim 10\%$ higher κ values than pattern 1. Data for samples with pattern 2 were therefore reduced by 10%. We estimate this to be the largest source of error, and thus expect the data to have an absolute error less than 10% throughout most of the temperature range. Small uncertainties in the slope of the thermometer calibration at the lowest temperatures result in a somewhat higher absolute error for $T<50$ mK. A pattern with three heaters was used to check for linearity of the measurement.

III. RESULTS

The thermal conductivity κ of four representative samples is shown in Fig. 3. The data exhibit a smooth change from a roughly linear variation above 1 K to a T^3 dependence at the lowest temperature. Except for the limiting T^3 rather than T^2 behavior at low temperatures, the magnitude and temperature dependence of the data are roughly similar to those of most glasses cooled from the melt. κ is strongly sample dependent, varying by a factor of ~ 5 at any given temperature, but for all samples it is greater than κ in Ref. 3. In contrast to those results, we find no correlation of κ with sample thickness.

We assume that the heat is carried by dispersionless thermal phonons whose variation of mean free path l with frequency is primarily responsible for the deviation of κ from a T^3 temperature dependence. We write[25,26]

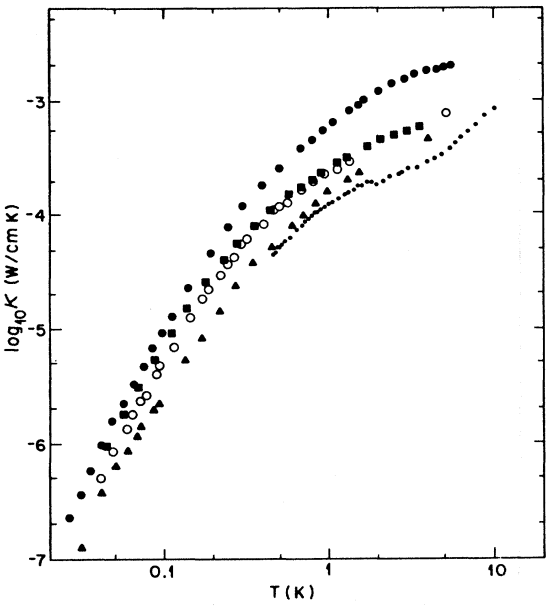

FIG. 3. Thermal conductivity of a-Ge for samples 1, 3, 4, 6, and LS (Ref. 3, small dots).

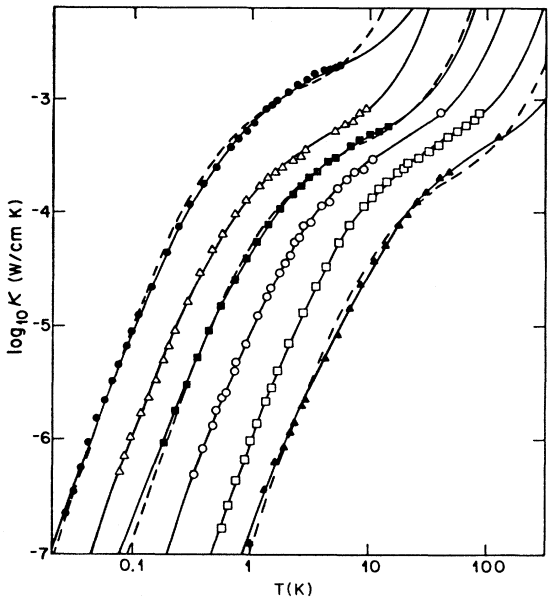

FIG. 4. Thermal conductivity of a-Ge for samples 1—6 with the symbols listed in Table I. For clarity, the data for samples 2—6 have been offset to higher temperatures by successive factors of 2. The solid lines represent Eq. (1) with the parameters given in the text and Table II. The dashed lines are best fits without two-level-system scattering.

$$\kappa(T)=\frac{\bar{v}}{3}\int_0^{\Omega_D} C(\Omega,T)l(\Omega,T)d\Omega\ , \tag{1}$$

with

$$l(\Omega)=(l_b^{-1}+l_R^{-1}+l_t^{-1})^{-1}+l_m\ . \tag{2}$$

$\Omega=\hbar\omega/k_B$ is the phonon frequency expressed in degrees Kelvin and $\bar{v}$ is a mode-averaged velocity. l_b represents scattering from the boundaries of the sample and is assumed to be frequency and temperature independent. l_R is the mean free path due to Rayleigh scattering from static density fluctuations, l_t is due to scattering from TLS, and l_m is a minimum mean free path. We have used $l_R=B/\Omega^m$ with $m=2$, 3, or 4, corresponding to planar, cylindrical, or spherical inhomogeneities, respectively, and

$$l_t^{-1}=A^{-1}\Omega\tanh(\Omega/2T)+(4A/\Omega+4/DT^3)^{-1}\ , \tag{3}$$

TABLE II. Parameters for the seven samples of Table I with $m=3$, and for sample 1 using $m=2(1_2)$ and $m=4(1_4)$. Units are the following: A (μm K), B (μm K^3), l_b (μm), and l_m (μm). χ^2/D_F is given for the fits with parameters as shown as well as for fits with parameters (not listed) which are optimized *without* two-level-system scattering.

Sample	A	B	l_b	l_m	χ^2/D_F	χ^2/D_F (no TLS)
1	450	721	516	103	0.8	2.7
2	435	234	383	490	0.6	1.2
3	201	206	593	253	0.2	1.5
4	313	210	282	380	0.6	1.3
5	385	211	149	294	0.3	1.1
6	60	170	301	167	1.3	7.5
LS	250	110				
1_2	990	170	600	4	11	
1_4	282	259	571	605	2.4	

where the first term represents resonant scattering and the second (much less important for our temperature range) represents relaxational scattering. Figure 4 shows the data for all six samples along the curves obtained by a least-squares fit of Eq. (1) with the parameters of Table II. We used $m=3$, a cutoff frequency $\Omega_D=315$ K, and an average velocity $\bar{v}=3.8\times10^5$ cm/sec, with the last two having been suggested by specific-heat measurements[6] above 1 K. The low values (<1) of the reduced χ^2 in Table II, where D_F is the number of degrees of freedom, indicate the high quality of the fits. The dashed lines in Fig. 4 are the results of refitting three of the samples *without* scattering from TLS. The obvious degradation in the quality of fits is reflected in the much larger values of χ^2/D_F, showing the importance of including two-level-system scattering. To illustrate the preference for $m=3$, curves with $m=2$ and 4 are also shown in Fig. 5 for sample 1, with A, B, l_b, and l_m modified to best fit the data. Good agreement is not possible with $m=2$. The agreement for $m=4$ is not as good as with $m=3$, both visually and statistically, and becomes much worse without the inclusion of TLS.[10] We also note that nearly twice as much two-level-system scattering is required with $m=4$ as with $m=3$. $l(\Omega)$ is plotted in Fig. 5 to illustrate its large variation with Ω. The large range of $l(\Omega)$ causes the fitting parameters to have low correlation with each other, as each then dominates the thermal conductivity over a quite distinct temperature interval. The parameters which we have fit to the data of Ref. 3 (Table II) are consistent with those for the present data. They are statistically meaningless, however, because of the high parameter correlation due to the small range of temperature.

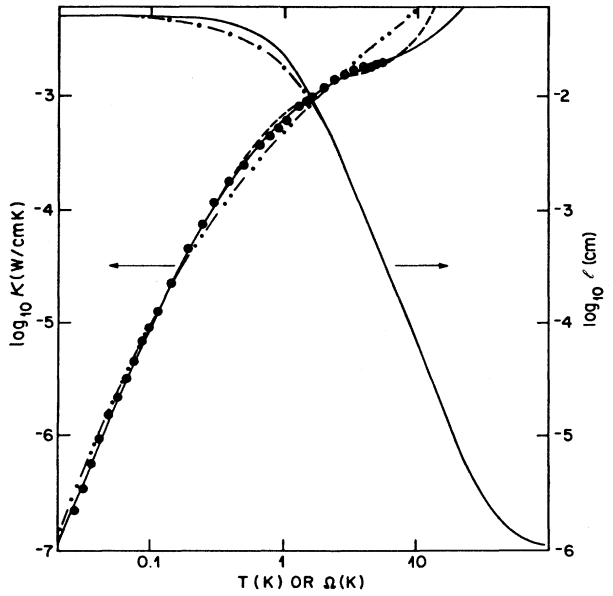

FIG. 5. Thermal conductivity of a-Ge sample 1. The solid line ($m=3$) is the same as the line in Fig. 4. The double-dotted—dashed and dashed lines represent Eq. (1) with $m=2$ and 4, respectively. The dashed-dotted and solid lines show $l(\Omega)$ for $T=0.1$ and 1 K, respectively.

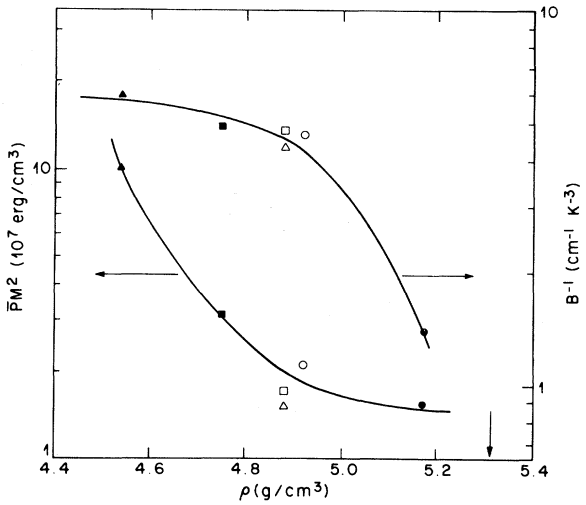

FIG. 6. Scattering strengths $\bar{P}M^2$ for TLS and B^{-1} for Rayleigh scattering from cylindrical inhomogeneities, as deduced from thermal-conductivity measurements on films of a-Ge of average mass density ρ. Symbols are given in Table I.

For most of the samples, l_b is 30—50 times the film thickness, implying highly specular reflection at the surfaces. This is consistent with their generally smooth visual appearance and with the absence of a size effect in the data. One exception is sample 5; its smaller value of l_b correlates with the rougher surface described above.

The scattering strength due to TLS is given by $\bar{P}M^2$, where $\bar{P}$ is the density of TLS which are effective in scattering phonons and M is their average matrix element. $\bar{P}M^2$ is related to A by[1]

$$\bar{P}M^2=\hbar\rho v^3/\pi k_B A \ . \tag{4}$$

$\bar{P}$ is a subset of n_0, the total density of TLS. We find an inverse correlation of both $\bar{P}M^2$ and the Rayleigh coefficient B^{-1} with the average mass density, shown in Fig. 6. These quantities change by factors of 7 and 5, respectively, as ρ varies by 12%. On the other hand, we find a lack of correlation of these parameters with impurity content.

IV. DISCUSSION

The Rayleigh scattering from cylindrical inhomogeneities implied by $m=3$ has support from x-ray measurements in similar material. Small-angle x-ray scattering[27] from evaporated thick films of a-Ge reveals cylinders approximately 30 Å in diameter and 2000 Å in length, with the long axis oriented parallel to the growth direction.[28–31] If the regions are voids, the cylinders occupy 1—2 % of the sample volume. (Therefore, as pointed out in Ref. 27, they can account for part but not all of the density deficit which in a-Ge can be as much as 30%.) We adapt an expression[32] for Rayleigh scattering from a line of missing atoms in a crystal, obtaining

$$l_R\Omega^3=4\hbar^3v^3/3k_B^3rd^2 \ , \tag{5}$$

where d is the average diameter of the cylinder and r is the porosity. For $d=30$ Å and $r=0.01$, we calculate $l_R\Omega^3=360\ \mu$m K^3, in remarkably good agreement with the values of B in Table II.

The criterion for Rayleigh scattering is that the phonon wavelength $\lambda\ (=2\pi\hbar v/k_B\Omega)\gtrsim d$. We can test whether this criterion is satisfied up to the highest frequency $\Omega_{\max}$ at which we are assuming that Rayleigh scattering dominates $l(\Omega)$. $\Omega_{\max}$ is calculated by setting $l_R=l_m$ to obtain $\Omega_{\max}=23$ K for typical values $B=200\ \mu$m K^3 and $l_m=160$ Å. At this frequency, $\lambda\approx 80$ Å, which easily satisfies the Rayleigh criterion if $d\approx 30$ Å.

The fact that the calculation of κ with $m=4$ yields almost as good agreement with the data as $m=3$ suggests that inhomogeneities with more spherical symmetry also exist. A separation into Ω^{-3} and Ω^{-4} contributions, however, is unwarranted in view of the competing scattering mechanisms and the broad spectrum of thermal phonons.

The physical interpretation of l_m is not straightforward. We have used it as the simplest mechanism to obtain the rise in κ which marks the upper temperature limit of the plateau and the onset of a quasi-T^3 dependence in most glasses. The sharp rise begins in a-Ge only at our highest temperatures, and therefore this parameter cannot be determined very accurately. It is only in this temperature range of 1—10 K that more complicated effects begin to be important, such as a nonquadratic phonon density of states[33] and phonon-phonon scattering.[34] l_m is therefore considered to be a zeroth-order approximation for a number of competing mechanisms which affect the data only at our highest temperatures.

The structure of a-Ge or a-Si films has been known for some time to be inhomogeneous. A low-density network was predicted[35] and then observed[36] in thin a-Si films. This morphology develops by columnar growth in thicker

films, with the spaces between columns presumably providing the long, thin cylinders discussed above. Associated with the cylinders or smaller voids are electronic defects, either dangling bonds or states in the band tails, that dominate the optical, electrical, and magnetic properties of this complicated material.[37] The number of defects per unit volume is generally observed to decrease as the overall mass density of the film approaches the crystalline density. Our results (Fig. 6) show that the number of cylinders also decreases with increasing mass density. Because of the inverse correlation of $\bar{P}M^2$ with density, we conclude that the TLS observed at low temperatures are associated with low-density regions in the material.[38] The rapid variation of B^{-1} only at high density indicates that the number and/or average diameter of the cylindrical inhomogeneities are relatively constant up to a density of $\sim 0.95\rho_c$. The rapid variation of $\bar{P}M^2$ at *low* density, on the other hand, suggests that the TLS are associated not with the cylinders but with the remaining low-density regions which account for most of the density deficit. It is just these regions about which the least is known at the present time. A number of papers have discussed the possibility of TLS existing in small voids[39] or on internal surfaces.[40]

It is interesting to compare the present results with previous reports of the low-temperature properties of *a*-Ge and *a*-Si, summarized in Table III in chronological order. C_p and κ of SiO_2 (Refs. 1 and 41) are included for comparison with a typical melt-quenched glass. Heat-capacity measurements[6] at $T > 1$ K showed no sign of TLS in sputtered samples of *a*-Ge, although later measurements[7] on evaporated material show a small contribution which is just above the noise level. The first clear evidence for TLS was found in the temperature-dependent dielectric constant[2] in sputtered *a*-Si. Thermal-conductivity measurements[3] in evaporated *a*-Ge were proposed as evidence of TLS, but as the present investigation shows, that claim is statistically meaningless because the data did not extend over a wide enough temperature range to analyze for various scattering mechanisms. Also present were the problems associated with the substrate as discussed above. Surface-acoustic-wave measurements[8] on sputtered *a*-Si showed no indication of TLS, but more recent measurements[4] on sputtered *a*-Ge with improved sensitivity show clear evidence for TLS with a scattering strength comparable to that found in our highest-density samples. This scattering strength is again below the detection limit of very recent, less sensitive measurements[42] using surface acoustic waves in sputtered *a*-Ge. Those authors[42] present evidence for TLS in sputtered films of *a*-GeO_x with $x=0.15$, 0.9, and 1.6, and suggest that the lower level of TLS observed previously[4] is associated with oxygen impurities. The present results at low but known oxygen levels[38] show this interpretation to be unlikely.

Thermal-conductivity measurements[9] in evaporated *a*-Ge (sample 1 of the present report) revealed a limiting T^3 behavior at low temperature which was interpreted qualitatively as evidence against TLS, while the present quantitative analysis indicates a small contribution from TLS in this sample. Recent measurements[5] of the heat capacity of *a*-Ge exhibited a quasilinear heat capacity which was markedly reduced upon annealing. The quasilinear term was attributed to spins, not to TLS, based on the argument that glasses show little change in two-level-system number density upon annealing, while the spin density is known to decrease with annealing. However, we point out that experiments which have studied the effect of annealing on TLS have been performed only on melt-quenched glasses, which are likely to have a much lower residual entropy (characteristic of thermal equilibrium at the glass transition temperature T_g) than films. The latter are deposited at lower temperature than T_g in a state which is much further from equilibrium. Thus we might expect, in general, a significant reduction in the number of TLS in films upon annealing. One can speculate that the as-prepared and annealed samples of Ref. 5 can be compared with the lowest- and highest-density samples of the present study. The quasilinear term in C_p is reduced upon annealing by approximately the same factor as the ratio of $\bar{P}M^2$ for our lowest- and highest-density films. It is difficult to compare the thermal-conductivity and heat-capacity results directly because $\bar{P} < n_0$, and M has not been measured in these materials. However, if we assume reasonable values ($M = 1$ eV and $\bar{P} = 0.1n_0$) we find that n_0 for our least dense sample ($n_0 = 4\times 10^{32}$ erg^{-1} cm^{-3}) is within a factor of 10 of the value deduced from the quasilinear C_p on unannealed samples (of unmeasured density). Whether or not spins make a significant contribution can only be determined by careful heat-capacity

TABLE III. Summary of experimental results on *a*-Ge and *a*-Si at low temperatures. SAW denotes surface acoustic wave. Letters after the material designate evaporated (e), sputtered (s), or bulk (b). The units of n_0 are 10^{32} erg^{-1} cm^{-3}; those of $\bar{P}M^2$ are 10^7 erg cm^{-3}. The entry for ϵ_1 is in units of esu eV^2.

Expt.	Material	n_0	$\bar{P}M^2$
C_p[a]	Ge(s)	<15	
C_p[b]	Ge(e)	~ 3	
ϵ_1[c]	Si(s)		1.7×10^{-4}
κ[d]	Ge(e)		>0
SAW[e]	Si(s)		<1.5
κ[f]	Ge(e)		~ 0
C_p[g]	Ge(e)	3—60	
SAW[h]	Ge(s)		1.35
SAW[i]	Ge(s)		$\lesssim 2$
κ[j]	Ge(e)		1.5—10
C_p[k]	SiO_2(b)	8	
κ[l]	SiO_2(b)		13

[a]Reference 6.
[b]Reference 7.
[c]Reference 2.
[d]Reference 3.
[e]Reference 8.
[f]Reference 9.
[g]Reference 5.
[h]Reference 4.
[i]Reference 42.
[j]This work.
[k]Reference 1.
[l]Reference 41.

measurements on well-characterized samples.

The present results appear to conflict with an early speculation[43] that the ideal, highly coordinated amorphous semiconductors *a*-Ge and *a*-Si should not contain TLS. This suggestion was made, however, before the inhomogeneous structure of these materials had been established. It is clear from the present results that films of *a*-Ge contain many sites at which tunneling can take place.

V. CONCLUSIONS

Previous reports of the low-temperature properties of *a*-Ge and *a*-Si have been in contradiction regarding the question of the existence of TLS. Some of the contradictions are undoubtedly related to the inhomogeneity of the material and to different preparation techniques. It is difficult to make comparisons among previous results because of insufficient characterization of the samples. In the present work we have varied the preparation conditions to obtain a wide range of samples which have been characterized by a number of different room-temperaure properties. The measurement of thermal conductivity at low temperatures allows us to detect the scattering of thermal phonons from both TLS and cylindrical inhomogeneities. The scattering strength of the cylindrical inhomogeneities agrees very well with an estimate based on small-angle x-ray scattering studies of microstructure in similar films. The inverse correlation of the scattering strength of TLS with average mass density indicates that the TLS are associated predominantly with the low-density regions of the material. The lack of correlation with impurity content suggests that the TLS observed here are intrinsic to *a*-Ge.

ACKNOWLEDGMENTS

We are grateful for many helpful suggestions by B. Golding, as well as useful discussions with J. J. Hauser, R. H. Willens, and B. G. Bagley. We thank T. Pignataro for developing the lifting technique, C. Doherty for preparing the first film, and K. B. Lyons, D. Aspnes, B. Prescott, J. P. Luongo, D. L. Malm, S. M. Vincent, P. Gallagher, D. Brasen, and J. E. Riley for assistance in characterizing the samples.

[1]*Amorhpous Solids: Low-Temperature Properties,* edited by W. A. Phillips (Springer, Berlin, 1981).

[2]B. Golding, J. E. Graebner, and W. H. Haemmerle, in *Amorphous and Liquid Semiconductors,* edited by W. E. Spear (Centre for Industrial Consultancy and Liaison, University of Edinburgh, Edinburgh, 1977), p. 367.

[3]H. v. Löhneysen and F. Steglich, Phys. Rev. Lett. 39, 1420 (1977).

[4]J. Y. Duquesne and G. Bellessa, J. Phys. C 16, L65 (1983).

[5]H. v. Löhneysen and H. J. Schink, Phys. Rev. Lett. 48, 1121 (1982).

[6]C. N. King, W. A. Phillips, and J. P. deNeufville, Phys. Rev. Lett. 32, 538 (1974).

[7]A. Cruz-Uribe and J. Trefny, in *Amorphous and Liquid Semiconductors,* Ref. 2, p. 175.

[8]M. von Haumeder, U. Strom, and S. Hunklinger, Phys. Rev. Lett. 44, 84 (1980).

[9]J. E. Graebner, B. Golding, and T. Pignataro, Bull. Am. Phys. Soc. 26, 418 (1981).

[10]J. E. Graebner and L. C. Allen, Phys. Rev. Lett. 51, 1566 (1983).

[11]R. D. Mathis Co., Long Beach, CA 90806.

[12]Fluorocarbon, Anaheim, CA 92803.

[13]Inficon, Leybold-Heraeus Co., East Syracuse, NY 13057.

[14]J. C. Knights, in *Amorphous and Liquid Semiconductors,* edited by W. Paul and M. Kastner (North-Holland, Amsterdam, 1980), p. 159.

[15]W. Paul, G. A. N. Connell, and R. J. Temkin, Adv. Phys. 22, 531 (1973).

[16]T. M. Donovan, W. E. Spicer, J. M. Bennett, and E. J. Ashley, Phys. Rev. B 2, 397 (1970).

[17]G. A. N. Connell, R. J. Temkin, and W. Paul, Adv. Phys. 22, 643 (1973).

[18]See for example, O. S. Heavens, *Optical Properties of Thin Solid Films* (Dover, New York, 1965).

[19]K. L. Chopra and S. K. Bahl, Phys. Rev. B 1, 2545 (1970).

[20]M. L. Theye, in *Amorphous and Liquid Semiconductors,* edited by J. Stuke and W. Brenig (Taylor and Francis, London, 1974), p. 479.

[21]T. M. Donovan, M. L. Knotek, and J. E. Fischer, in *Amorphous and Liquid Semiconductors,* Ref. 20, p. 549.

[22]M. Zavetova, S. Koc, and J. Zemek, Czeck. J. Phys. B 22, 429 (1972).

[23]M. L. Knotek and T. M. Donovan, Phys. Rev. Lett. 30, 652 (1973).

[24]Wedge-bonding machine Model 7400A, West-Bond, Inc., Orange, CA 92665.

[25]M. P. Zaitlin and A. C. Anderson, Phys. Rev. B 12, 4475 (1975).

[26]J. Jäckle, in *The Physics of Non-Crystalline Solids,* edited by G. H. Frischat (Transtech, Rockport, Mass., 1976), p. 568.

[27]G. S. Cargill, Phys. Rev. Lett. 28, 1372 (1972).

[28]J. J. Hauser and A. Staudinger, Phys. Rev. B 8, 607 (1973).

[29]N. G. Nakhodkin, A. I. Shaldervan, A. F. Bandamid, and S. P. Chenakin, Thin Solid Films 34, 21 (1976).

[30]A Staudinger and S. Nakahara, Thin Solid Films 45, 125 (1977).

[31]S. V. Krishnaswamy, R. Messier, Y. S. Ng, T. T. Tsong, and S. B. McLane, in *Amorphous and Liquid Semiconductors,* Ref. 14, p. 531.

[32]P. G. Klemens, Proc. Phys. Soc. London, Sect. A 68, 1113 (1955).

[33]N. Bilir and W. A. Phillips, Philos. Mag. 32, 113 (1975).

[34]D. P. Jones, N. Thomas, and W. A. Phillips, Philos. Mag. B 38, 271 (1978).

[35]F. L. Galeener, Phys. Rev. Lett. 27, 1716 (1971).

[36]T. M. Donovan and K. Heinemann, Phys. Rev. Lett. 27, 1794 (1971).

[37]See many articles in Refs. 2, 14, 20, and 21.

[38]We have considered the possibility that the TLS are associated with oxygen which is known to diffuse rapidly into films upon exposure to air. [See, for example, M. L. Knotek, J.

Vac. Sci. Technol. 12, 117 (1975)]. However, the similarity of the scattering strengths of TLS in sample 5 (1.5 at. % oxygen), sample 2 (0.2 at. %), and sample 4 (0.05 at. %) strongly suggests that the TLS are not associated with oxygen impurities.

[39]M. H. Cohen and G. S. Grest, Phys. Rev. Lett. 45, 1271 (1980).

[40]J. C. Phillips, Phys. Rev. B 24, 1744 (1981).

[41]D. P. Jones and W. A. Phillips, Phys. Rev. B 27, 3891 (1983).

[42]K. L. Bhatia and S. Hunklinger, Solid State Commun. 47, 489 (1983).

[43]W. A. Phillips, J. Low Temp. Phys. 7, 351 (1972).